Level structure of the odd mass Pr isotopes: Levels of $^{143}Pr_{84}$ populated in the beta decay of ^{143}Ce

D. F. Kusnezov
National Superconducting Cyclotron Laboratory, Department of Physics and Astronomy, Michigan State University, East Lansing, Michigan 48824

D. R. Nethaway and R. A. Meyer
Nuclear Chemistry Division, Lawrence Livermore National Laboratory, Livermore, California 94550
(Received 12 April 1989)

We have studied the levels of ^{143}Pr populated in the beta decay of ^{143}Ce using singles and Compton suppression gamma-ray spectroscopy techniques. We determined a value of 33.10±0.05 h for the half-life of ^{143}Ce. In contrast to previous studies, we find no evidence for low-energy negative-parity levels in the decay of ^{143}Ce to ^{143}Pr. In addition we have performed calculations in the framework of the interacting boson-fermion model, which compare well with the level structure of ^{143}Pr. These calculations have been extended to the heavier Pr isotopes.

I. INTRODUCTION

Recently, we have shown that symmetry models can account for the drastic change in low-energy-level structure of the $N=59$ isotones.[1] Similar behavior is encountered in the $Z=59$ isotopes in the region from shell closure at $N=82$ to deformation beyond $N=90$. Such drastic changes in the level structure are difficult to account for in any model, and we attempt to account for it in using fermion boson model. The interacting boson-fermion model (IBFM) and the particle truncated quadrupole phonon model (PTQM) have been shown to be equivalent fermion-boson models,[2] in which the even-even core is first described and then the odd nucleon is coupled to the IBM/TQM core. Here, we compare the capability of the fermion boson models to account for the low-energy levels of the $Z=59$ nucleus ^{143}Pr, for which we have experimentally determined the nature of the low-energy levels using gamma-ray spectroscopy techniques. Using the ^{143}Pr quasiparticle interaction strengths we examine the predictions for the level structure of $^{145,147}Pr$. In a companion paper[3] we extend our comparison of the fermion-boson description with the results of our experimental spectroscopy study of ^{145}Pr, where the systematic structure of the wave functions of the odd mass Pr isotopes are studied.

Our experimental half-life and gamma-ray spectroscopy measurements, in combination with the original conversion electron measurements,[4,5] establish the low-energy-level structure of ^{143}Pr. The dearth of prior literature on the decay of ^{143}Ce and the levels of ^{143}Pr has been recently reviewed in Nuclear Data Sheets (NDS) by Peker,[6] who adopted our gamma-ray spectroscopy results[7] for the gamma-rays resulting from the decay of ^{143}Ce.

II. EXPERIMENTAL MEASUREMENTS

In order to perform a complete set of measurements, we used two separate methods to produce sources of ^{143}Ce. In the first, sources of ^{143}Ce were made by irradiating ^{236}U with neutrons from the Lawrence Livermore National Laboratory's (LLNL's) insulated core transformer (ICT). The second method used Cerium oxide enriched 99% ^{142}Ce. These samples were irradiated in the core hole position of LLNL's pool type reactor (LPTR).

For the measurement of the half-life of ^{143}Ce, six samples were prepared from separate irradiations of ^{236}U. Cerium was extracted from the mixed fission products and purified by standard Nuclear Chemistry Division (NCD) radiochemical procedures, including a rare-earth separation on a cation-exchange column. The samples were counted with a NaI(Tl) crystal with lower and upper discriminators set at 200 and 400 keV, respectively. A beryllium absorber of 354 mg/cm^2 was used. The decay of the samples was followed using the NCD's automated half-life measurement system, which we have described elsewhere.[8] The counting data were analyzed with a least-squares computer program PEANUTS, in which we used two components: the unknown, ^{143}Pr, and the single-known impurity, ^{144}Ce, whose half-life value[9] was fixed at 284 d.

For the gamma-ray measurements of ^{143}Ce, two types of sources were used. In one, Ce was isolated by rare-earth cation-exchange column separation from mixed fission products of a neutron irradiation of ^{236}U at the LPTR. These samples were placed into a mass-separator crucible and mass separated. The resulting sources of mass separated ^{143}Ce were used to make precision intensity measurements with the NCD spectrometers. Samples used in the Compton suppression spectrometer required more intense sources, which were produced by neutron irradiation of the enriched ^{142}Ce in the LPTR. These sealed sources had no chemical or mass separation.

The sources were measured using a gamma-ray coincidence spectrometer and several different Ge(Li) spectrometers at source-to-detector distances ranging from 10 to 100 cm. During these experiments spectra were accumulated with no absorber between the source and detec-

tor as well as with a variety of absorbers. The low-intensity high-energy gamma rays present were measured by counting with 12.4 mm of lead absorber between the source and detector while the source was 10 cm from the detector. The energy calibration was performed by counting the ^{143}Ce with a series of known multigamma-ray standards.[7] Also, because an accurate knowledge of the relative intensities was needed, a series of counting experiments were performed in which the ^{143}Ce was measured simultaneously with the standard sources such as ^{152}Eu and ^{133}Ba. This allowed reconfirmation of the precise shape of the detector efficiency curve at low energies at the time of measurement, which was important in setting a precise ratio of the 57–293-keV gamma-ray intensities.

III. RESULTS

We present the results of our half-life measurements in Table I and our gamma-ray measurements in Table II. The precision measurement of gamma-ray energies and intensities were listed in an earlier report on multigamma-ray standards.[7] These values were adopted in the recent NDS for the 143 mass chain.[6] The values given in Table II are our more complete set and include the more recent measurements of the precise ratio between the 57- and 293-keV gamma-ray intensities, which is important in setting the beta population of the ^{143}Pr ground state (g.s.). Recently, Gehrke[10] has determined the absolute intensity of the 293-keV gamma ray, whose multipolarity mixture of 37±4% $E2$ was accurately measured earlier by Gelletly *et al.*[11] As adopted in NDS,[6] we use Gehrke's value of 42.8±0.4 gamma rays per 100 decays of ^{143}Ce. However, because of the difficulty of measurement and the differing values of the 57-keV transition that were reported, we exclude the values given for the 57-keV transition (two values are given in Ref. 10). Further, as noted below, our gamma-ray values and the decay scheme in combination with Gehrke's absolute inten-

TABLE I. Measurement of the half-life of ^{143}Ce

Expt.[a]	Pts.[b]	Interval (days)		Half-life (days)
		Begin	End	
1	29	2.8	7.7	1.3887(64)
2	25	2.9	10.7	1.3802(35)
3	59	2.9	10.8	1.3875(25)
4	19	2.8	9.9	1.3875(25)
5	77	2.9	22.7	1.3802(14)
6	63	2.8	23.9	1.3765(15)
Final value = 1.379(2) days[c] or 33.10(5) h				

[a]This column gives the experiment number.
[b]This column gives the number of experimental points taken in the respective measurement.
[c]This value is the one sigma value. For use in metrology, we suggest use of the two sigma value of 33.1±0.1 h.

TABLE II. Gamma-ray energies, intensities, and assignments for the decay of ^{143}Ce to levels of ^{143}Pr.

Energy (keV)	Intensity[a] (relative)	Assignment from	to
57.356(7)	274(8)	57	g.s.
122.4(1)	0.20(7)	1060	937
139.742(17)	1.8(1)	490	350
197.6(2)	0.06(3)	937	721
231.550(2)	48(1)	721	490
272.9(2)	≤0.2	1060	787
293.266(2)	1000(3)	350	57
338.3(2)	0.02(1)	1060	721
350.619(3)	75.5(6)	350	g.s.
357.8(2)	0.014(5)	848	490
371.292(29)	0.58(6)	721	350
389.64(2)	0.85(4)	740	350
416.57(10)	0.16(3)	1156	740
432.999(6)	3.71(7)	490	57
438.43(8)	0.10(2)	1160	721
446.02(9)	0.35(7)	1060	614
447.45(2)	1.40(6)	937	490
490.368(5)	50.5(5)	490	g.s.
497.81(2)	1.04(6)	848	350
523.0(5)	0.04(1)	1014	490
556.87(1)	0.74(4)	614	57
569.91(9)	0.12(4)	1061	490
587.20(2)	6.23(6)	937	350
594.5(4)	≤0.05	1381	787
614.22(3)	0.28(3)	614	g.s.
664.571(15)	133(1)	721	57
670.12(7)	0.19(4)	1160	490
675.5(5)	0.02(1)	1397	721
682.82(9)	0.20(4)	740	57
709.59(5)	0.20(3)	1060	350
721.929(13)	126(1)	721	g.s.
729.87(8)	0.07(1)	787	57
767.70(6)	0.074(8)	1381	614
787.40(9)	0.06(1)	787	g.s.
791.07(2)	0.31(1)	848	57
806.34(2)	0.67(2)	1156	350
809.98(2)	0.73(2)	1160	350
880.46(1)	24.1(2)	937	57
891.47(7)	0.19(2)	1381	490
907.1(1)	0.03(1)	1397	490
937.82(1)	0.61(3)	937	g.s.
956.9(1)	0.03(1)	1014	g.s.
1002.85(1)	1.76(4)	1060	57
1014.3(3)	0.03(1)	1014	g.s.
1031.22(3)	0.47(2)	1381	350
1046.78(4)	0.28(2)	1397	350
1060.22(2)	0.85(3)	1060	g.s.
1103.25(2)	9.7(1)	1160	57
1160.58(6)	0.056(7)	1160	g.s.
1324.478(28)	0.037(1)	1381	57
1340.1(1)	0.072(3)	1397	57
1382(1)	0.009(3)	1381	g.s.

[a]Intensities are given relative to the 293.268-keV gamma-ray intensity being taken as 1000 units. For conversion to absolute intensity we adopt Gehrke's value (Ref. 10) for the absolute intensity of the 293.368-keV gamma-ray. This leads to a conversion factor of 0.0428(4).

sity for the 293-keV transition lead to a g.s. beta transition intensity of $\leq 0.2\%$. This beta intensity value results in a $\log f_1 t$ value ≥ 10. Such a value is consistent with the known hindrances of unique first-forbidden (UFF) beta transitions when cluster configurations are involved;[12] such as here where the ^{143}Pr with a $\frac{7}{2}^+$ $(1g_{7/2})$ g.s. is populated by a UFF transition from the ^{143}Ce with a $\frac{3}{2}^-$ cluster configuration of $\{(1f_{7/2})^3\}$. Further, we note that use of Gehrke's value for the 57-keV transition gives an unrealistic value of $>100\%$ for the cumulative beta intensity. In Table III we give the conversion coefficients and multipolarities for selected transitions in ^{143}Pr. The conversion electron intensities were determined from the reports of Bashandy and co-workers[4,5] by using the reported conversion coefficients and the gamma-ray intensities quoted by Bashandy in each paper. In general, we adopt values derived from the second work,[5] in which Bashandy used an iron-free double focusing beta-ray spectrometer. We note that, although claiming to use values from the first work[4] and only noting the second work,[5] the conversion coefficients listed in NDS correspond to those extracted from the second work, which was published at a later date.

Several multipolarities, derived from the conversion-electron intensities obtained from the work of Bashandy and our gamma-ray intensities, require further comment. First, some transitions were originally suggested to have $E1$ multipolarity and as a consequence, resulted in evidence for the surprising occurrence of low-energy negative parity levels. As can be seen in Table III, our reanalysis does not find any evidence for the presence of $E1$ transitions in the ^{143}Ce to ^{143}Pr decay scheme. Of particular importance is the 389-keV transition. This was originally suggested to possess $E1$ multipolarity. However, inspection of the published data and spectra leads to the conclusion that the intense $L351$-keV transition ($E_e \sim 345$ keV) obfuscates any determination of the low-intensity $K389$ line because it occurs at approximately the same energy ($E_e \sim 347$ keV) as the $K389$ line. In Table III we show the energy difference between the transition energy we determine and those reported by Bashandy. As shown by the values in the square brackets in column 1 of Table III, the values in the energy range 400–900 keV are consistently 2–4 keV higher in energy for those reported by Bashandy. Because of this, we associate the K line reported by Bashandy at 810 keV with the 806 keV transition and not the 810 keV transition observed in the gamma-ray measurements. Also, we find no evidence for any $E0$ component in either the 1031- or 1046-keV transitions as suggested in the recent NDS report.[6] When we include all errors associated with these transitions, we find that, although the values are higher than expected, the conversion coefficients are, within error, consistent with an $M1$ multipolarity. Other features and inconsistencies are given as footnotes in Table III.

In Fig. 1 we show the levels of ^{143}Pr that we deduce from our gamma-ray singles and coincidence spectra following ^{143}Ce beta decay. The level assignments and $\log ft$ values are given in Table IV. The $\log ft$ and $\log f_1 t$ values were calculated using our half-life value of 33.10 h, our gamma-ray intensities, the calculated conversion

TABLE III. Conversion coefficients for transitions in ^{143}Pr.

E_t[a,b] (keV)	Intensity[c] (relative)	Conversion coefficients	Mult./Comment
231[1]	400(60)[d]	0.085(13)	$E2$(+M1?)
293[0]	5200(400)[d]	0.053(4)	$M1+37\%/E2$[e]
351[0]	185(23)[d]	0.25(2)	Fiducial $E2$
371[3]	3.3(5)[f]	0.041(6)	$M1$
389[2]	≥ 0.7[g]	$\geq 0.008(2)$	$(M1/E2)$/[g]
432[4]	8.0(6)	0.022(40)	$M1$
44X[h]	2.9(9)[d]	0.017(5)	Both $M1/E2$/[h]
490[3]	72(9)[d]	0.015(2)	$M1/E2$
556[2]	0.5(2)	0.007(4)	$E2$ (+M1?)
587[4]	5.8(7)[c]	0.010(1)	$M1$
664[4]	85(13)[d]	0.0065(10)	$M1$ (+E2?)
721[4]	88(8)[c]	0.0071(7)	$M1$
806[3]	0.29(4)[c]	0.0044(6)	$M1+E2$/[i]
880[2]	11(2)	0.0047(4)	$M1$
937[2]	0.13(5)[c]	0.0022(8)	$E2$
1003[1]	0.49(11)	0.0028(6)	$M1$
1031[1]	0.17(4)	0.0037(12)	$M1$ No $E0$/[j]
1046[2]	0.11(3)	0.0040(15)	$M1$ No $E0$/[j]
1060[1]	0.18(5)	0.0022(6)	$M1$ (+E2?)
1103[1]	2.2(4)[d]	0.0023(4)	$M1$

[a]The value in square brackets that follows the transition energy (E_t) is the energy difference between our values and those reported by Bashandy (Refs. 4 and 5).

[b]We find no evidence for several lines reported in both studies by Bashandy (Refs. 4 and 5), i.e., photopeaks at 218, 291, 314, 408, 509, 790, and 1275 keV.

[c]The K conversion-electron intensities were calculated using the gamma-ray intensities and conversion coefficients reported in each of the two works by Bashandy. Several values reported in Bashandy's first work (Ref. 4) are as much as a factor of 10 larger than those in the latter work (Ref. 5). Except where noted, we have adopted the values reported in the later work. We note that although Peker (see NDS, Ref. 6) claims to use the values of Bashandy's earlier work, the values quoted for the conversion coefficients, do in fact, correspond to use of the values reported in the later work.

[d]This is the average value of those given in Bashandy's two reports, which in the case of the 293- and 350-keV transitions, is the same value.

[e]The 37% $E2$ was measured by Gelletly, Geiger, and Graham (Ref. 11).

[f]This value is adopted from Bashandy's latter report (Ref. 5).

[g]The $L351$ ($E_e \sim 345$ keV) severely interferes with the $K389$ ($E_e \sim 347$ keV) transition. Hence a reliable value should not be expected for this K conversion coefficient. This was not recognized in previous reports, including the Nuclear Data Sheets (Ref. 6), and led to the erroneous assignment of an $E1$ multipolarity for the 389-keV transition.

[h]Bashandy reports a 448-keV line. We take this to be the sum of the 446- and 447-keV transitions which we observe.

[i]This electron line was misassigned to the 809-keV transition by Peker in Nuclear Data Sheets. Assignment to the $K809$ line is more consistent with the energy differences of all the other transitions (see values in square brackets in column 1).

[j]We do not find evidence for any $E0$ components in this transition as suggested in NDS. If all errors are included, the conversion coefficient value, although large, is consistent with an $M1$ multipolarity.

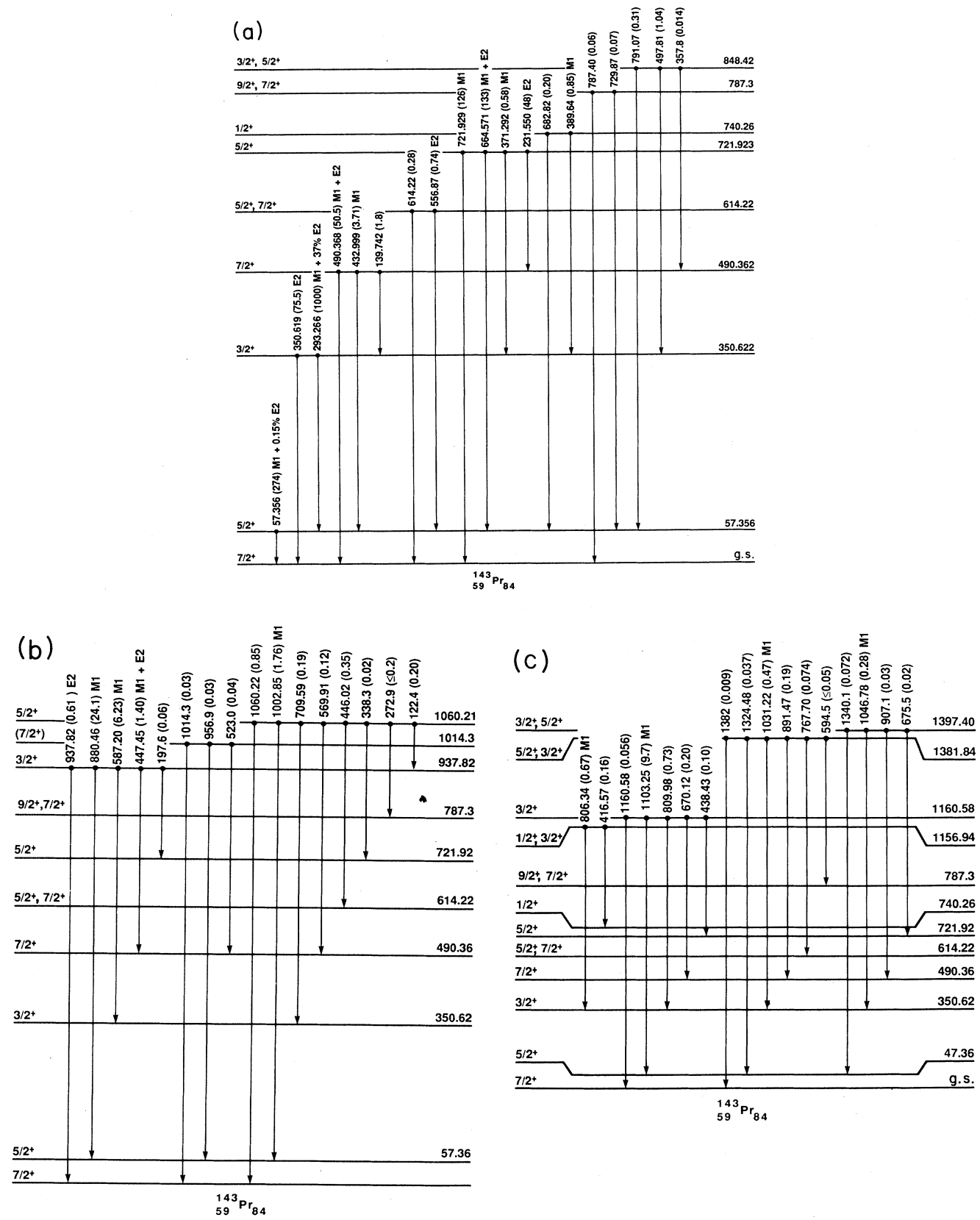

FIG. 1. Level scheme for ^{143}Pr deduced from the decay of 33.10 h ^{143}Ce. (a) Levels up to 900 keV; (b) levels from 900 to 1100 keV; (c) levels above 1100 keV. (See Table IV for logft and logf_1t values for the level's population in the beta decay of 33.10 h. ^{143}Ce with g.s. spin parity of $\frac{3}{2}^-$.)

coefficients, the absolute gamma-ray intensities for the 293-keV transition determined by Gehrke, a beta-decay energy value of 1461.6±1.9 as given by Wapstra and Audi,[13] and the tables of Gove and Martin.[14] The unique first-forbidden beta transitions to the three $\frac{7}{2}^+$ states, which are suggested to be populated in the beta-decay of $\frac{3}{2}^-$ ^{143}Ce, all have logf_1t values of ≥ 10. As we discussed above, this is consistent with the known UFF strength[12] for transitions from cluster configurations such as the $\frac{3}{2}^-\{(1f_{7/2})^3\}$ g.s. of ^{143}Ce. The levels at (spin-parity in parenthesis) 0 ($\frac{7}{2}^+$), 57 ($\frac{5}{2}^+$), 350 ($\frac{3}{2}^+$), 490 ($\frac{7}{2}^+$), 721 ($\frac{5}{2}^+$), 937 ($\frac{3}{2}^+$), 1060 ($\frac{5}{2}^+$), and 1160 ($\frac{3}{2}^+$) have been assigned spin-parity values by Peker in his recent compilation in Nuclear Data Sheets. Two of the levels, 1381 and 1397 keV, were assigned as $\frac{3}{2}^+$ by Peker on the basis of population of $\frac{3}{2}^+$ levels by deexciting transitions which had $E0$ components. As given in Table III (see footnote j) we cannot find firm evidence for an $E0$ component for the transitions in question, and hence, have added the possibility of a $\frac{5}{2}^+$ value to both levels. However, based on the level properties we give a preference of $\frac{5}{2}^+$ for the 1381-keV level and $\frac{3}{2}^+$ for the 1397 keV level. Similarly, based on their logft values, deexcitation patterns and the transitions that populate them we suggest a spin-parity value of $\frac{1}{2}^+$ and $\frac{3}{2}^+$ for the 740- and 1014-keV levels, respectively. We note that for higher energy levels in the decay scheme a $\frac{7}{2}^+$ value is excluded because the logf_1t value becomes unrealistically low. Because of their population (logft values) and depopulation (branching ratios, multipolarities, etc.) properties, several levels can have their spin-parity values restricted. These are the levels at (spin-parity in parenthesis) 614 ($\frac{5}{2}^+$, $\frac{7}{2}^+$), 787 ($\frac{9}{2}^+$, $\frac{7}{2}^+$), and 1157 ($\frac{1}{2}^+$, $\frac{3}{2}^+$) keV.

TABLE IV. Spin-parity and logft values for levels of ^{143}Pr populated in the beta decay of ^{143}Ce.

Energy (keV)	logft [a]	Spin parity	Comment
g.s.	[>10]	$\frac{7}{2}^+$	b
57	7.70	$\frac{5}{2}^+$	b
350	7.18	$\frac{3}{2}^+$	b
490	[10.2]	$\frac{7}{2}^+$	b
614	10.0	$\frac{5}{2}^+, \frac{7}{2}^+$	c
721	7.11	$\frac{5}{2}^+$	b
740	9.61	$\frac{1}{2}^+$	d
787		$\frac{9}{2}^+, \frac{7}{2}^+$	e
848	9.18	$\frac{3}{2}^+, \frac{5}{2}^+$	c
937	7.58	$\frac{3}{2}^+$	b
1014	[10.5]	$\frac{7}{2}^+$	c
1060	8.08	$\frac{5}{2}^+$	b
1156	8.37	$\frac{1}{2}^+, \frac{3}{2}^+, \frac{5}{2}^+$	c
1160	7.25	$\frac{3}{2}^+$	b
1381	6.59	$\frac{5}{2}^+, \frac{3}{2}^+$	c
1397	6.59	$\frac{3}{2}^+, \frac{5}{2}^+$	c

[a]Where appropriate the logf_1t value is given in square brackets.
[b]Spin-parity value assigned by Peker in NDS (Ref. 6).
[c]We assign this value on the basis of the level's branching ratios, multipolarities of transitions populating and depopulating the level, and its beta population.
[d]The 397-keV transition, which deexcites this level, was previously thought to be of $E1$ character. However, our investigations show that this transition has $M1$ multipolarity. Consequently, the spin-parity value suggested for this level is based on the character of the transition populating the level, the lack of transition to ground state, and multipolarity of its deexciting 389-keV transition.
[e]Within experimental error, this level is not directly populated in the beta decay of ^{143}Ce, which has a g.s. spin-parity value of $\frac{3}{2}^-$.

IV. DISCUSSION

We have performed systematic IBFM calculations on the level structure of the odd mass Pr isotopes ^{143,145,147}Pr using the IBFM equivalent model PTQM. Although we are primarily concerned with the level structure of ^{143}Pr, multiparameter studies are better suited to systematic studies of several neighboring nuclei. In this description, the ^{143,145,147}Pr are described as proton quasiparticles coupled to the collective quadrupole excitations of the even-even ^{142,144,146}Ce cores, respectively. In the first step we determined the core parameters by describing the experimentally known levels of the even-even core nuclei in the TQM frame-work. The TQM Hamiltonian, which is equivalent to the IBM Hamiltonian,[19] has the standard form

$$H_{\rm TQM}=h_1\hat{N} + h_2\{[b^\dagger b^\dagger]^{(0)}\sqrt{(N-\hat{N})(N-\hat{N}-1)}+\text{h.c.}\} + h_3\{[b^\dagger b^\dagger\tilde{b}]^{(0)}\sqrt{N-\hat{N}}+\text{h.c.}\} + \sum_{L=0,2,4} h_{4,L}\{[b^\dagger b^\dagger]^{(L)}[\tilde{b}\tilde{b}]^{(L)}\}^{(0)} .$$

Here $b_\mu^\dagger$ and $\tilde{b}_\mu$ are the quadrupole phonon creation and annihilation operators and $\hat{N}$ is the number operator. The bosons were taken as paired particles counted from the $Z=50$ closed shell. The total boson number N was 5, 6, and 7 for ^{142,144,146}Ce, respectively. The strengths of the anharmonic terms h_1, h_2, h_3, and h_{4L} were chosen to best describe the low-energy structure of the Ce cores. The theoretical results are compared to the experimentally known low-energy levels of the even-even Ce in Fig. 2. Using the transformation between these anharmonic strengths and the more standard IBM parameters, it is straightforward to verify the consistency of our parameters with other IBM studies in this shape transitional region. In Table V we compare our Ce parameters to the IBM parameters of Snelling[15,16] for Nd.

Using the even-even core parameters, we have calculated the positive parity levels in ^{143}Pr as well as the heavier Pr isotopes. In this step, a proton quasiparticle was coupled to each of the even-even Ce cores. The coupling is described by the PTQM Hamiltonian:[17]

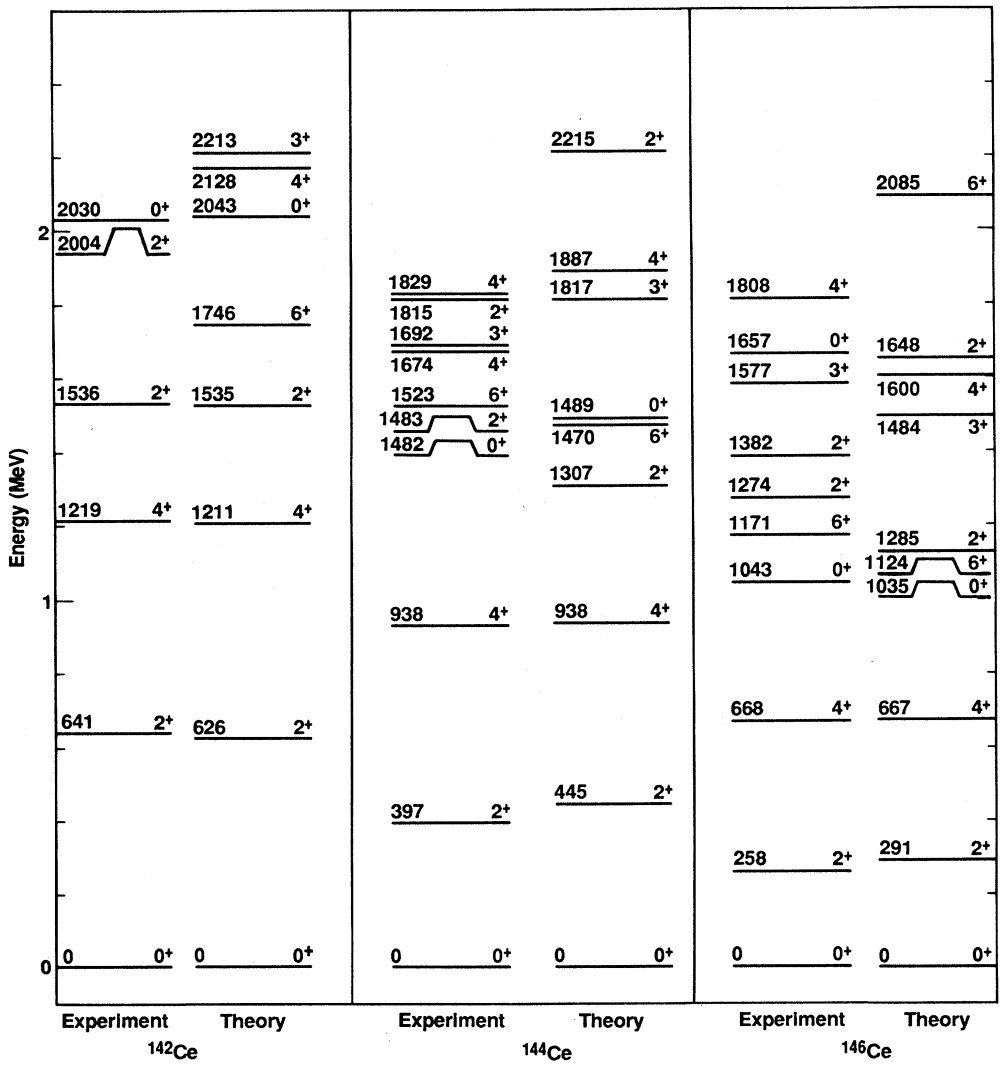

FIG. 2. Comparison of the levels of the even-even core nuclei ^{142}Ce, ^{144}Ce, and ^{146}Ce with the experimentally known levels (data taken from Ref. 9).

$$H_{\mathrm{PTQM}}=H_P+H_{\mathrm{TQM}}+H_{\mathrm{PVI}}\ .$$

Here H_P is the quasiparticle Hamiltonian, H_{TQM} is the Hamiltonian used for the even-even core, and H_{PVI} describes the interaction between the odd quasiparticle and the quadrupole phonons. H_{PVI} is chosen in the standard form[17]

$$H_{\mathrm{PVI}}=\sum_j A_j[(b^\dagger\tilde{b})^{(0)}(c_j^\dagger\tilde{c}_j)^{(0)}]^{(0)}+\sum_{j_1,j_2}\Gamma_{j_1,j_2}[\hat{Q}^{(2)}(c_{j_1}^\dagger\tilde{c}_{j_2})^{(2)}]^{(0)}+\sum_{j_1,j_2,j_3}\Lambda_{j_1j_2j_3}:[(c_{j_1}^\dagger\tilde{b})^{(j_3)}(\tilde{c}_{j_2}b^\dagger)^{(j_3)}]^{(0)}:\ ,$$

TABLE V. Comparison of parameters used for even-even core calculations

Isotope	h_1	h_2	h_3	h_{40}	h_{42}	h_{44}
^{142}Ce	0.58	−0.15	−0.14	0.45	0.10	−0.10
^{144}Ce	0.45	−0.13	−0.15	0.35	0.03	0
^{146}Ce	0.38	−0.09	−0.15	0.28	0	0.05
^{144}Nd	0.72	−0.03	−0.09	0.27	0.08	−0.15
^{146}Nd	0.52	−0.03	−0.09	0.27	0.08	−0.15
^{148}Nd	0.38	−0.06	−0.09	0.22	−0.03	0.12
^{150}Nd	0.25	−0.05	−0.10	0.22	−0.02	0.07

TABLE VI. PTQM parameters for ^{143,145,147}Pr.

Isotope	Γ_0	Λ_0	A_0	$v^2(g_{7/2})$	$v^2(d_{5/2})$	$v^2(d_{3/2})$	ϵ_{gd} (MeV)[a]	ϵ_{dd} (MeV)[b]
^{143}Pr	1.17	0.60	0	0.746	0.380	0.024	0.094	1.80
^{145}Pr	1.17	0.60	0	0.748	0.380	0.024	0.098	1.78
^{147}Pr	1.17	0.60	0.05	0.751	0.379	0.025	0.101	1.76

[a]This column gives the energy difference adopted between the $g_{7/2}$ and $d_{5/2}$ orbitals.
[b]This column gives the energy difference adopted between the $d_{3/2}$ and $d_{5/2}$ orbitals.

with

$$\hat{Q}^2_\mu = b^\dagger_\mu \sqrt{N-\hat{N}} + \sqrt{N-\hat{N}}\,\tilde{b}_\mu - \frac{\sqrt{7}}{2}(b^\dagger \tilde{b})^{(2)}_\mu ,$$

$$A_j = A_0\sqrt{5}(2j+1) ,$$

$$\Gamma_{j_1 j_2} = \Gamma_0\sqrt{5}(u_{j_1}u_{j_2} - v_{j_1}v_{j_2})\langle j_1 \| Y_2 \| j_2 \rangle ,$$

$$\Lambda_{j_1 j_2 j_3} = -2\Lambda_0 \left[\frac{5}{2j_3+1}\right]^{1/2} (u_{j_1}v_{j_3} + v_{j_1}u_{j_3}) \times (u_{j_3}v_{j_2} + v_{j_3}u_{j_2})\langle j_3 \| Y_2 \| j_1 \rangle \langle j_3 \| Y_2 \| j_2 \rangle .$$

Here u_j^2 and v_j^2 are the BCS occupation probabilities and $c^\dagger_{jm}$ and $\tilde{c}_{jm}$ are the quasiparticle creation and annihilation operators, respectively. The BCS occupation probabilities and quasiparticle energies were estimated from the work of Kisslinger and Sorensen.[18] The monopole term A_0 is relatively unimportant, as it effectively rescales the boson number operator resulting in overall compression or expansion of the spectra. Hence the main features of the experimental spectra were described with only the dynamical (Γ_0) and exchange (Λ_0) interactions. The two parameters Γ_0 and Λ_0 were determined by fitting to the experimental energy spectrum of ^{143}Pr. These parameters were further constrained by requiring that the same parameters also describe the known low-energy spectrum of ^{145}Pr and ^{147}Pr. With this prescription we found it essential to include the $d_{3/2}$, $d_{5/2}$, and $g_{7/2}$ orbitals in the calculation. Without the $d_{3/2}$ orbital, a consistent set of parameters could not be found that describe the low-energy $\frac{3}{2}^+$ levels known in ^{145}Pr and ^{147}Pr. As we showed elsewhere,[19] the need to include the $d_{3/2}$ orbital can be accounted for because the PTQM includes a nonspin flip term that brings about drastic lowering in energy of the $j-2$ partners of particular particle j states. Thus including the $d_{3/2}$ orbital brings about explicit configuration mixing through the nonspin flip term.

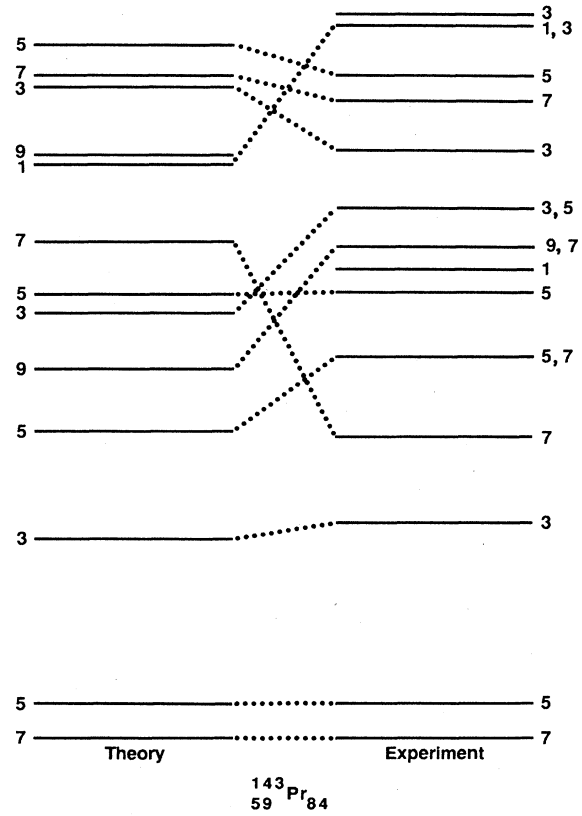

FIG. 3. Comparison of levels calculated within the IBFM/PTQM model compared with our experimentally determined levels. The levels are labeled by $2J$, twice the spin.

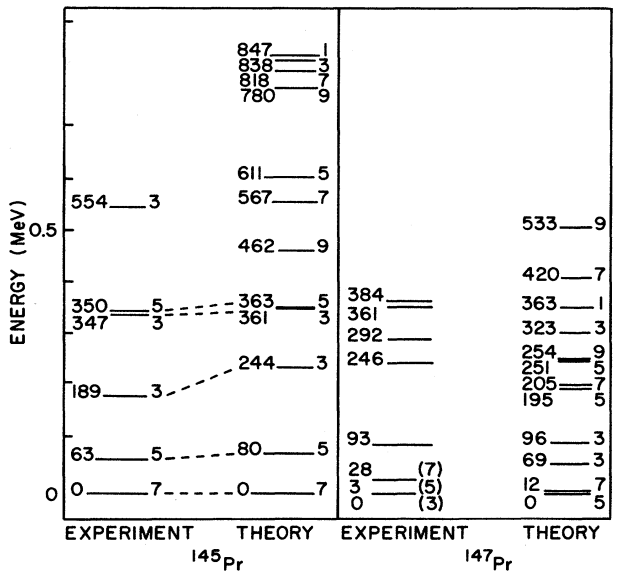

FIG. 4. Comparison of experimental levels to levels calculated within the IBFM/PTQM model for ^{145,147}Pr using the ^{143}Pr quasiparticle interactions Λ_0 and Γ_0. An additional monopole strength of $A_0=0.05$ was used for ^{147}Pr. The levels are labeled by $2J$, twice the spin.

The PTQM parameters that we determined are given in Table VI. In Fig. 3 we compare the calculated levels of ^{143}Pr with those that are experimentally known, and in Fig. 4 the comparison to the heavier odd mass Pr isotopes[3,20] using the same quasiparticle interactions is shown. A small monopole interaction strength of $A_0 = 0.05$ MeV was used for ^{147}Pr to better reproduce the low energy level density since there are no firm spin-parity assignments. This description of the odd-mass Pr isotopes does reproduce the qualitative systematics of the low energy levels in these transitional nuclei. Although there is insufficient firm spin-parity assignments for detailed comparison, the calculations do replicate the general density of levels. Further, since the same quasiparticle coupling strengths are used for these isotopes, it is evident that the even-even Ce cores are responsible for the change in the level systematics in the odd-mass Pr isotopes. We defer a detailed study of the wave functions to our companion article in which the experimental structure of ^{145}Pr is presented.[3]

In concluding we stress that, as differentiated from prior studies,[4–6] we find no evidence for low-energy low-spin negative parity levels in ^{143}Pr, which is in contrast to the heavier Pr isotopes where possible octupole coupled states occur at low energy.[3]

ACKNOWLEDGMENTS

We wish to thank B. Mendoza in the Nuclear Chemistry Division (NCD) for his assistance and Prof. V. Paar, University of Zagreb, for his critical review of the calculations. One of us (D.K.) wishes to thank the NCD for its support during the on-site phase of this work. This work was performed under the auspices of the U. S. Department of Energy by the Lawrence Livermore National Laboratory under Contract No. W-7405-Eng-48 and also in part by the National Science Foundation under Grant No. 87-14432.

[1]R. A. Meyer, S. Brandt, and V. Paar, Inst. of Phys. Conf. Ser. **88**, 454 (1988).
[2]R. A. Meyer and V. Paar, *Nuclear Structure, Reactions and Symmetries* (World Scientific, Singapore, 1986).
[3]E. Baum, J. D. Robertson, P. F. Mantica, Jr., S. H. Faller, C. A. Stone, W. B. Walters, R. A. Meyer, and D. F. Kusnezov, Phys. Rev. C **39**, 1514 (1989).
[4]E. Bashandy, S. G. Hanna, and A. Abd. El-Haliem, J. Phys. Soc. Jpn. **22**, 960 (1967).
[5]E. Bashandy, Z. Naturforsch. **26a**, 683 (1971).
[6]L. K. Peker, Nucl. Data **48**, 753 (1986).
[7]R. A. Meyer and T. N. Massey, Int. J. Appl. Rad. Isot. **34**, 1073 (1983).
[8]R. J. Nagle and R. A. Meyer, Phys. Rev. C **16**, 747 (1977).
[9]*Table of Isotopes*, 7th ed., edited by C. M. Lederer and V. S. Shirley (Wiley, New York, 1978).
[10]R. J. Gehrke, Int. J. Appl. Radiat. Isot. **33**, 355 (1982).
[11]W. Gelletly, J. S. Geiger, and R. L. Graham, Phys. Rev. **168**, 1336 (1968).
[12]R. A. Meyer, E. A. Henry, C. F. Smith, J. E. Fontanilla, S. M. Lane, H. G. Hicks, R. J. Nagle, and O. G. Lien III, Lawrence Livermore National Laboratory Report No. UCRL-85261, 1987 (unpublished).
[13]A. H. Wapstra and G. Audi, Nucl. Phys. **A432**, 1 (1985); 55 (1985).
[14]N. B. Gove and M. J. Martin, Nucl. Data. Tables **10**, 206 (1971).
[15]D. M. Snelling, Ph. D. thesis, Sussex University, 1982.
[16]D. M. Snelling and W. D. Hamilton, J. Phys. G **9**, 111 (1983).
[17]V. Paar, S. Brandt, L. F. Canto, G. Leander, and M. Vouk, Nucl. Phys. **A378**, 41 (1982).
[18]L. Kisslinger and R. A. Sorensen, Rev. Mod. Phys. **35**, 853 (1963).
[19]Y. Tokunaga, H. Seyfarth, R. A. Meyer, O. W. B. Schult, H. G. Börner, G. Barreau, H. R. Faust, K. Schreckenbach, S. Brandt, V. Paar, M. Vouk, and D. Vretenar, Nucl. Phys. **A439**, 425 (1985).
[20]W. B. Walters, private communication.